Two-color QCD at nonzero quark-number density

J. B. Kogut
Department of Physics, University of Illinois, 1110 West Green Street, Urbana, Illinois 61801-3080

D. K. Sinclair
HEP Division, Argonne National Laboratory, 9700 South Cass Avenue, Argonne, Illinois 60439

S. J. Hands and S. E. Morrison
Department of Physics, University of Wales Swansea, Singleton Park, Swansea SA2 8PP, United Kingdom
(Received 24 May 2001; published 8 October 2001)

We have simulated two-color four-flavor QCD at nonzero chemical potential μ for quark number. Simulations were performed on 8^4 and $12^3\times 24$ lattices. Clear evidence was seen for the formation of a colorless diquark condensate which breaks quark number spontaneously, for $\mu > \mu_c \sim m_\pi/2$. The transition appears to be second order. We have measured the spectrum of scalar and pseudoscalar bosons which shows clear evidence for the expected Goldstone boson. Our results are in qualitative agreement with those from effective Lagrangians for the potential Goldstone excitations of this theory.

DOI: 10.1103/PhysRevD.64.094505 PACS number(s): 11.15.Ha

I. INTRODUCTION

QCD at finite quark/baryon-number density at zero and at finite temperature describes nuclear matter. Nuclear matter at high temperatures (and possibly densities) was certainly present in the early universe. Neutron stars consist of dense cold nuclear matter. The BNL Relativistic Heavy Ion Collider (RHIC) and the CERN heavy-ion program promise to produce hot nuclear matter in the laboratory. Calculating the properties of high density nuclear matter could predict if and where strange matter could be produced. Any method that can be used to determine the properties of nuclear matter could be adapted to nuclear physics calculations.

Finite quark-number density is best achieved by introducing a chemical potential μ for quark number, and using the grand-canonical partition function. Unfortunately, this renders the Euclidean-time fermion determinant complex, with a real part which can change sign. Standard lattice simulations, which rely on importance sampling, fail in this case. Attempting to circumvent these problems by using canonical (fixed quark number) ensembles fails except at high temperatures [1] because of sign problems.

Until a simulation method is found that avoids these difficulties, it is useful to study models which exhibit *some* of the properties of QCD at high μ. Now it is expected that, at zero temperature, nuclear matter undergoes a phase transition at μ of order one-third the mass of the nucleon. It has been proposed that at still higher μ the ground state is characterized by a diquark condensate [2–6]. Such a condensate would not only cause spontaneous breaking of the baryon number, but would also spontaneously break color. Since color is a gauge symmetry, such breaking is realized in the Higgs mode. Thus nuclear matter would become a color superconductor at high μ.

For this reason we have simulated 2-color QCD, i.e., SU(2) Yang-Mills theory with fermion matter fields (''quarks'') in the fundamental representation of $SU(2)_{color}$, and finite μ. As well as having color confinement this theory does exhibit diquark condensation as we shall demonstrate in this paper, but for $\mu > \mu_c \sim m_\pi/2$, since the diquark ''baryons'' in the same multiplet as the pions, also have mass m_π. For $\mu \lesssim m_\pi$ the phenomenon is describable as a rotation of the condensate from the chiral to the diquark direction as predicted by effective Lagrangian analyses [7]. Unlike in true (3-color) QCD, the diquark condensates are colorless, the broken symmetry is realized in the Goldstone mode, and there is no color superconductivity, but rather superfluidity, as in liquid ^{3}He. Despite this, we shall later argue that this theory is more similar to 2-flavor QCD than one might think (see Sec. IV).

Since 2-color QCD has a non-negative determinant and pfaffian, even at nonzero μ, standard simulation methods can be used. We use the hybrid molelcular-dynamics method and simulate the theory with 4 flavors of staggered quarks [8]. Pfaffian simulations of a 4-fermion model, including a diquark source term, have been reported in [9]. We have run simulations at a moderately large quark mass and an intermediate gauge coupling on 8^4 and $12^3\times 24$ lattices, i.e., at zero temperature. We measured order parameters including the chiral and diquark condensates, the quark-number and energy densities, and the Wilson line (Polyakov loop). The larger lattice allowed us to observe finite size effects and, more importantly, to measure the scalar and pseudoscalar meson and diquark masses, which include all the potential Goldstone bosons in the theory. Preliminary results from these simulations were reported Ref. [10]. The extension of these calculations to finite temperature was reported in a recent letter [11]. This work builds on early work with 8 quark flavors which presented far less conclusive results [12]. Previous studies of diquark condensation in this model with various numbers of flavors have either used the approximation where $\lambda = 0$ in the updating algorithm [13] (as does [12]), or been in the strong gauge-coupling regime [14].

Section II introduces the staggered-fermion lattice port of 2-color QCD. The results of our simulation are presented in

Sec. III. Section IV gives our conclusions and indicates future avenues of research.

II. LATTICE 2-COLOR QCD

Because in 2-color QCD fundamental quarks and antiquarks lie in the same representation of $SU(2)_{color}$ the flavor symmetry group for N_f flavors is enlarged from $SU_L(N_f)\times SU_R(N_f)\times U_V(1)$ to $SU(2N_f)$. The pattern of chiral symmetry breaking is $SU(2N_f)\to Sp(2N_f)$ rather than the usual $SU_L(N_f)\times SU_R(N_f)\to SU_V(N_f)$ [15,7]. 3-color QCD with 1 staggered quark (4 continuum flavors) has a $U_V(1)\times U(1)_\varepsilon$ flavor symmetry. For 2 colors this is enhanced to $U(2)$ [12]. Chiral or quark-number symmetry breaking [the chiral and diquark condensates lie in the same U(2) multiplet] occurs according to the pattern $U(2)\to U(1)$.

The quark action for 2-color QCD with one staggered quark is

$$S_f=\sum_{sites}\left\{\bar{\chi}[\not{D}(\mu)+m]\chi+\frac{1}{2}\lambda[\chi^T\tau_2\chi+\bar{\chi}\tau_2\bar{\chi}^T]\right\} \quad (1)$$

where $\not{D}(\mu)$ is the normal staggered covariant finite difference operator with μ introduced by multiplying the links in the $+t$ direction by e^{μ} and those in the $-t$ direction by $e^{-\mu}$. The superscript T stands for transposition. Note that we have introduced a gauge-invariant Majorana mass λ which explicitly breaks quark-number symmetry. Such an explicit symmetry-breaking term is needed to observe spontaneous symmetry breaking on a finite lattice. We shall be interested in the limit $\lambda\to 0$. Integrating out these fermion fields yields

$$pfaffian\begin{bmatrix}\lambda\tau_2 & \mathcal{A}\\ -\mathcal{A}^T & \lambda\tau_2\end{bmatrix}=\sqrt{\det(\mathcal{A}^\dagger\mathcal{A}+\lambda^2)} \quad (2)$$

where

$$\mathcal{A}\equiv\not{D}(\mu)+m. \quad (3)$$

We note that $\mathcal{A}^\dagger\mathcal{A}+\lambda^2$ is positive definite for finite λ. Hence the pfaffian never vanishes and thus, by continuity arguments never changes sign and can be chosen to be positive. Note that $\det(\mathcal{A})$ has been shown to be positive in [16]. Denoting the 2×2 matrix in Eq. (2) by $\mathcal{M}$ we have seen that its determinant is the determinant of a positive definite matrix and thus can be used directly in our simulations. To do this we define $\tilde{\mathcal{M}}$ by

$$\tilde{\mathcal{M}}=\begin{bmatrix}1 & 0\\ 0 & \tau_2\end{bmatrix}\mathcal{M}\begin{bmatrix}\tau_2 & 0\\ 0 & 1\end{bmatrix} \quad (4)$$

so that

$$\tilde{\mathcal{M}}=\begin{bmatrix}\lambda & \mathcal{A}\\ -\mathcal{A}^\dagger & \lambda\end{bmatrix} \quad (5)$$

and

$$\tilde{\mathcal{M}}^\dagger\tilde{\mathcal{M}}\to\begin{bmatrix}\mathcal{A}^\dagger\mathcal{A}+\lambda^2 & 0\\ 0 & \mathcal{A}\mathcal{A}^\dagger+\lambda^2\end{bmatrix}. \quad (6)$$

We note that $\det[\mathcal{A}\mathcal{A}^\dagger+\lambda^2]=\det[\mathcal{A}^\dagger\mathcal{A}+\lambda^2]$. Because we are now dealing with the matrix $\tilde{\mathcal{M}}^\dagger\tilde{\mathcal{M}}$ we can use the hybrid molecular dynamics method with "noisy" fermions [8] to simulate this theory. Here, although we generate Gaussian noise with both upper and lower components, we keep only the upper components of the pseudo-fermion field to calculate $\det[\mathcal{A}^\dagger\mathcal{A}+\lambda^2]$, which means that we only need to invert $\mathcal{A}^\dagger\mathcal{A}+\lambda^2$ at each update. Keeping only half the components of the pseudo-fermion field is entirely analogous to keeping only the fermion fields on even sites in normal QCD simulations. The square root of Eq. (2) is obtained by inserting a factor of $\frac{1}{2}$ in front of the fermion term in the stochastic action in the standard manner.

We now give a brief discussion of symmetry breaking in this model. This is covered in more detail in [12]. At $\mu=m=\lambda=0$, the $U(2)$ symmetry will break spontaneously. Two directions in which it will choose to break are of particular interest. The first is where it breaks to give a nonzero chiral condensate $\langle\bar{\chi}\chi\rangle$. There will be 3 Goldstone bosons corresponding to the 3 broken generators of $U(2)$. These states and their corresponding $U(2)$ generators are

$$\begin{aligned}\mathbf{1}&\Rightarrow\bar{\chi}\epsilon\chi\\ \sigma_1&\Rightarrow\chi^T\tau_2\chi-\bar{\chi}\tau_2\bar{\chi}^T\\ \sigma_2&\Rightarrow\chi^T\tau_2\chi+\bar{\chi}\tau_2\bar{\chi}^T.\end{aligned} \quad (7)$$

σ_3 remains unbroken. The second is where $U(2)$ breaks to give a nonzero diquark condensate $\frac{1}{2}\langle\chi^T\tau_2\chi+\bar{\chi}\tau_2\bar{\chi}^T\rangle$. This time the 3 Goldstone bosons and corresponding generators are

$$\begin{aligned}\mathbf{1}&\Rightarrow\chi^T\tau_2\epsilon\chi+\bar{\chi}\tau_2\epsilon\bar{\chi}^T\\ \sigma_2&\Rightarrow\bar{\chi}\chi\\ \sigma_3&\Rightarrow\chi^T\tau_2\chi-\bar{\chi}\tau_2\bar{\chi}^T.\end{aligned} \quad (8)$$

σ_1 remains unbroken. When $\mu\neq 0$ only 2 Goldstone bosons remain, $\chi^T\tau_2\epsilon\chi+\bar{\chi}\tau_2\epsilon\bar{\chi}^T$ and $\chi^T\tau_2\chi-\bar{\chi}\tau_2\bar{\chi}^T$. When in addition $m\neq 0$, only the latter state remains a Goldstone boson. A more detailed study of the patterns of symmetry breaking can be performed in terms of an effective Lagrangian for the Goldstone modes as in [7]. The only difference is that the effective field, denoted Σ in that work, here belongs to a symmetric 2×2 tensor representation of $U(2)$ rather than to the antisymmetric $2N_f\times 2N_f$ representation of $SU(2N_f)$ of the continuum case.

One can see the remnant $U(1)$ symmetry when $\lambda\to 0$ by allowing λ to become complex. The Majorana mass term in Eq. (1) then becomes $\frac{1}{2}[\lambda\chi^T\tau_2\chi+\lambda^*\bar{\chi}\tau_2\bar{\chi}^T]$. λ^2 is replaced by $|\lambda|^2$ in the pfaffian.

Although the 2-flavor theory would be of more interest in the continuum, we have chosen to simulate the 4-flavor theory because this represents a single staggered quark species and thus has well defined symmetries and a well defined spectrum at all lattice spacings. Unlike the 8-flavor case simulated in [12] it probably does have a sensible continuum limit.

III. SIMULATIONS OF 2-COLOR, 4-FLAVOR LATTICE QCD

We have simulated 2-color QCD with 1 staggered quark species (4 continuum flavors) on 8^4 and $12^3\times 24$ lattices. The simulations reported here are all at $\beta=4/g^2=1.5$ which is roughly the β_c for the finite temperature transition on an $N_t=4$ lattice [17]. This first set of simulations has been performed with quark mass $m=0.1$ in lattice units. These simulations are currently being repeated at $m=0.025$, where the smaller pion mass will give a richer spectrum of Goldstone and pseudo-Goldstone bosons and where a larger portion of the relevant phase diagram should be described by effective Lagrangians. (We have also performed some zero temperature simulations at $\beta=1.0$ and $m=0.05$. This has been reported in our finite temperature/finite μ letter [11].) Since we wished to take the limit $\lambda\to 0$, we needed $\lambda\ll m$. The values we chose were $\lambda=0.01$ and $\lambda=0.02$ for $m=0.1$. (At low μ's we also ran at $\lambda=0$.)

The smaller lattice was used to map out the interesting range of μ values, measuring order parameters including the diquark condensate $\langle\chi^T\tau_2\chi\rangle$, the chiral condensate $\langle\bar{\chi}\chi\rangle=\langle\bar{\psi}\psi\rangle$, and the number density $j_0=(1/V)(\partial\ln S_f/\partial\mu)$. In addition to measuring these quantities on the larger lattice, we also calculated the spectrum of potential Goldstone bosons. The length of each ''run'' was 2000 molecular dynamics time units. dt had to be chosen as low as 0.005 for $\lambda=0.01$ and $0.4<\mu\leqslant 0.975$. In Fig. 1 we have plotted the diquark condensate as a function of μ at each λ for both lattice sizes.

Since we are interested in the limit where the symmetry-breaking parameter $\lambda\to 0$, we have performed a linear extrapolation of the diquark condensate to $\lambda=0$. Note that the effective Lagrangian calculations [7], and lower statistics simulations we performed at $m=0.05$ [11] where we used 3 λ values, suggest that linear extrapolations are the correct approach for λ sufficiently small, except at μ_c. The results of these extrapolations are plotted in Fig. 2. What we first notice is that for $\mu\leqslant 0.2$, the extrapolated diquark condensate is small enough that we can believe that it should be zero. For $\mu\geqslant 0.35$ it is clearly nonzero. The points at $\mu=0.3$ would appear to show finite size rounding were it not for the fact that the 8^4 and $12^3\times 24$ points are so close together. We think it more likely that $\mu=0.3$ is so close to the transition that the linear extrapolation has broken down. We therfore conclude that the system undergoes a phase transition at $\mu=\mu_c\approx 0.3<m_\pi/2=0.37622(5)$. If this holds true, the fact that μ_c is less than $m_\pi/2$ would indicate that the diquark ''baryons'' do not exist as free particles but bind into ''nuclear'' matter. Over the range $0.35\leqslant\mu\leqslant 0.6$, the condensate increases with a curvature consistent with a critical index $\beta_{qq}<1$ (the tree level effective Lagrangian analysis predicts the mean field result $\beta_{qq}=\frac{1}{2}$). Since the condensate starts to decrease soon after $\mu=0.6$, the scaling region is

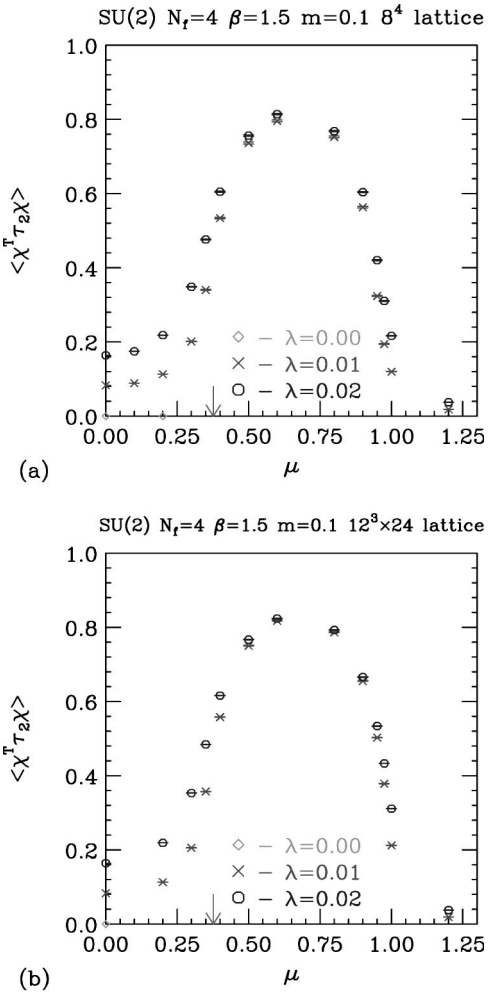

FIG. 1. $\langle\chi^T\tau_2\chi\rangle$ as a function of μ: (a) on an 8^4 lattice and (b) on a $12^3\times 24$ lattice. The arrow is at $\mu=m_\pi$.

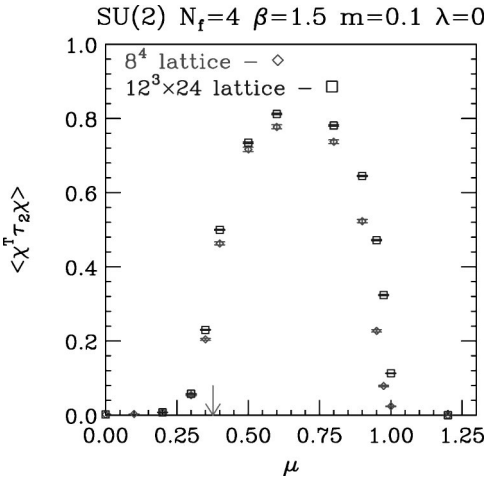

FIG. 2. $\langle\chi^T\tau_2\chi\rangle$ extrapolated to $\lambda=0$ as a function of μ on both 8^4 and $12^3\times 24$ lattices.

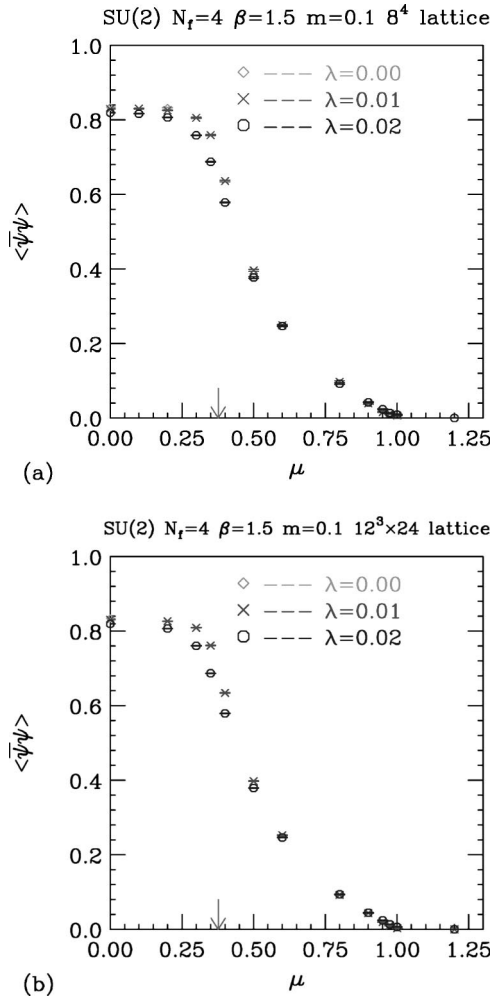

FIG. 3. $\langle\bar{\psi}\psi\rangle$ as a function of μ: (a) on an 8^4 lattice and (b) on a $12^3\times 24$ lattice.

narrow and it would require more points to even try to extract this critical index. For $\mu \gtrsim m_\pi$, the condensate starts to decrease, approaching zero for large μ, which would appear to be a saturation effect. In fact, Fig. 2 suggests that the condensate vanishes for $\mu > \mu_s \approx 1$, indicating a saturation phase transition. We shall have more to say about this later. Note that this decrease in the condensate with μ is not predicted by the effective Lagrangian analysis, which is only expected to be valid for small μ and m_π. This is not surprising if it is indeed a saturation effect. Saturation is a result of the fermi statistics of the quarks, and should not be seen in a model which only considers the system's bosonic excitations.

We now turn to a consideration of the chiral condensate, $\langle\bar{\chi}\chi\rangle = \langle\bar{\psi}\psi\rangle$. This is plotted in Fig. 3 for our 2 different lattice sizes. In the $\lambda \to 0$ limit, this is expected to be constant at its $\mu = 0$ value for $\mu < \mu_c$. These plots are consistent with this expectation. Above μ_c, effective Lagrangian studies predict that the condensate merely rotates from the chiral direction to the diquark direction, so that the magnitude of the condensate, i.e., $\sqrt{\langle\bar{\chi}\chi\rangle^2 + \langle\chi^T\tau_2\chi\rangle^2}$, should remain constant and independent of λ. Since the diquark condensate increases up to $\mu \sim m_\pi$, this means that the chiral condensate should fall, as it does. It, however, continues to fall past this point, because of saturation effects, appearing to vanish for $\mu > \mu_s$. To test the prediction that the principal effect for $\mu < m_\pi$ is merely a rotation, we have tabulated $\sqrt{\langle\bar{\chi}\chi\rangle^2 + \langle\chi^T\tau_2\chi\rangle^2}$ in Table I. We see that, for $\mu \leqslant 0.6$, the magnitude of the condensate is approximately constant and independent of λ, so that the main effect is a rotation of the condensate from the direction of chiral symmetry breaking to that of quark-number breaking. For $\mu \geqslant 0.8$, it decreases with increasing μ approaching zero for large μ.

TABLE I. Magnitude of the condensate $\sqrt{\langle\bar{\chi}\chi\rangle^2 + \langle\chi^T\tau_2\chi\rangle^2}$ as functions of μ and λ on a $12^3\times 24$ lattice. Errors are not quoted but they are in the next or a subsequent digit after the least significant quoted digit.

	|Condensate|	
μ	$\lambda = 0.01$	$\lambda = 0.02$
0.000	0.835	0.836
0.200	0.834	0.836
0.300	0.835	0.839
0.350	0.841	0.840
0.400	0.845	0.846
0.500	0.850	0.856
0.600	0.856	0.860
0.800	0.792	0.799
0.900	0.657	0.667
0.950	0.503	0.534
0.975	0.379	0.433
1.000	0.212	0.311
1.200	0.019	0.038

In Fig. 4 we plot the quark-number density $j_0 = (1/V)(\partial \ln S_f/\partial\mu)$ as a function of μ for our 2 lattices. j_0 is consistent with zero as $\lambda \to 0$ for $\mu < \mu_c$. (Note effective Lagrangians predict that it vanishes quadratically with λ in this region.) Above μ_c it increases with increasing μ approaching the saturation value of 2 (1 staggered quark field of each color per site, the maximum value allowed by Fermi statistics) for large μ. Note that Fig. 4 suggests that $j_0 = 2$ for $\mu > \mu_s$ with μ_s consistent with that predicted from the condensates. This indicates that it is this saturation which causes the condensates to vanish for $\mu > \mu_s$. It also tells us that this transition is an artifact of the finite lattice spacing and would recede to infinite μ in the continuum limit.

For the chiral condensate and quark number density presented above, we note excellent agreement between the 8^4 and $12^3\times 24$ measurements which indicates that finite size effects are well under control. For the diquark condensate the values for the 2 lattice sizes are close enough for $\mu \leqslant 0.8$ that we feel confident in assuming that the $12^3\times 24$ values are excellent estimates of the infinite volume numbers. For $\mu > 0.8$, while the shapes of the 2 curves are similar, the finite size effects are clearly large. Fortunately, since the behavior of the system in this region is dominated by saturation effects which are a lattice artifact, we do not need good quantitative measurements here.

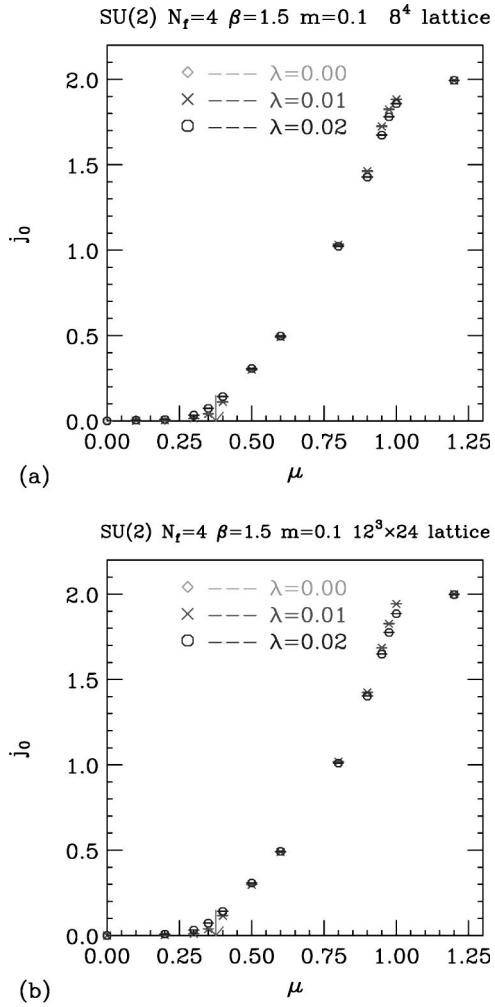

FIG. 4. Quark-number density as a function of μ: (a) on an 8^4 lattice and (b) on a $12^3\times 24$ lattice.

On the $12^3\times 24$ lattice we have measured the propagators for all the potential Goldstone bosons, both scalar and pseudoscalar, using a single noisy point source for the connected propagators and multiple (5) noisy point sources for the disconnected propagators. We have measured both diagonal and off-diagonal zero momentum propagators.

In Fig. 5 we show the masses from fitting the propagator for the diquark state produced by applying the operator $\chi^T\tau_2\chi-\overline{\chi}\tau_2\overline{\chi}^T$ to the vacuum, to the form

$$P_G(T)=A\{\exp[-m_G T]+\exp[-m_G(N_t-T)]\}, \qquad (9)$$

valid for large temporal separations T. As argued in Sec. II, this is the expected Goldstone boson for $\mu>\mu_c$ and $\lambda=0$. The effective Lagrangian approach indicates that, in the low μ phase, this mass should be quadratic in λ, while in the high μ phase, it should vanish as $\sqrt{\lambda}$. We have performed extrapolations based on this and plotted them in the figure. Note that with only 2 λ values, we cannot test these assumptions directly, but since this behavior is expected on fairly general grounds, we assume it and check that it produces sensible results. For the 3 points closest to the transition μ

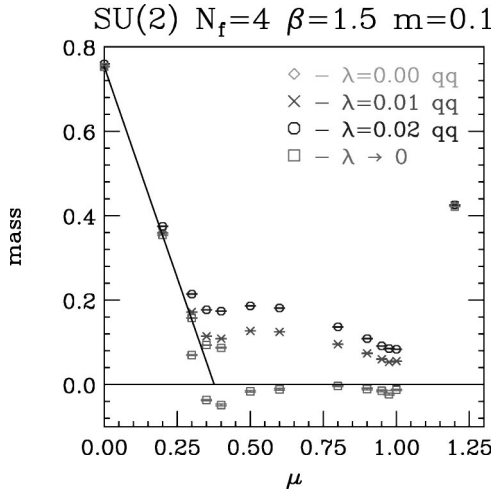

FIG. 5. Mass of the diquark state expected to become a Goldstone boson in the diquark condensed phase as a function of μ for $\lambda=0.1$ and $\lambda=0.2$. The line is the expected linear behavior expected for the symmetric phase. Also included are the points at $\lambda=0$, $\mu=0$ and $\lambda\to 0$ extrapolations.

$=0.3,0.35,0.4$, we have performed both extrapolations. For $\mu<m_\pi/2$ and $\lambda=0$, we expect

$$m_G=m_\pi-2\mu \qquad (10)$$

with $m_\pi=m_\pi\,(\mu=0)$. We see that for $\mu\leqslant 0.3$, the points obtained from quadratic extrapolation lie on this straight line, the point at $\mu=0.35$ is close to the line and that for $\mu=0.4$ lies above this line. All points for $0.35\leqslant\mu\leqslant 1.0$ obtained by square root extrapolation are negative. The points at $\mu=0.35,0.4$ show the most significant negative values (although both are greater than -0.05), and should be considered as transitional. The other points are so close to zero that one can easily attribute the difference as being due to a combination of the systematic errors in extracting masses from point source propagators and higher order terms in the extrapolation. Thus our results are consistent with a transition to a phase with a massless (Goldstone) scalar diquark at $\mu\approx m_\pi/2=0.37622(5)$, as expected. Finally the large value of this diquark mass at $\mu=1.2$ is further indication that the system has passed through the saturation phase transition.

We now turn to consideration of the other potential Goldstone bosons of the theory. Since at this quark mass m_π^2 is relatively large, we concentrate on those states which are expected to have masses of order m_π or less over the range of interest. For this reason, we consider the pion itself. For $\mu<\mu_c$, its mass should remain constant at m_π, and it is created by the operator $\overline{\chi}\epsilon\chi$. For $\mu>\mu_c$, it is expected to mix with the pseudoscalar diquark state created from the vacuum by the operator $\chi^T\tau_2\epsilon\chi+\overline{\chi}\tau_2\epsilon\overline{\chi}^T$. Rather than trying to diagonalize the propagator over these 2 states, we have instead calculated the diagonal propagators for each of these states separately. These we fit to the form

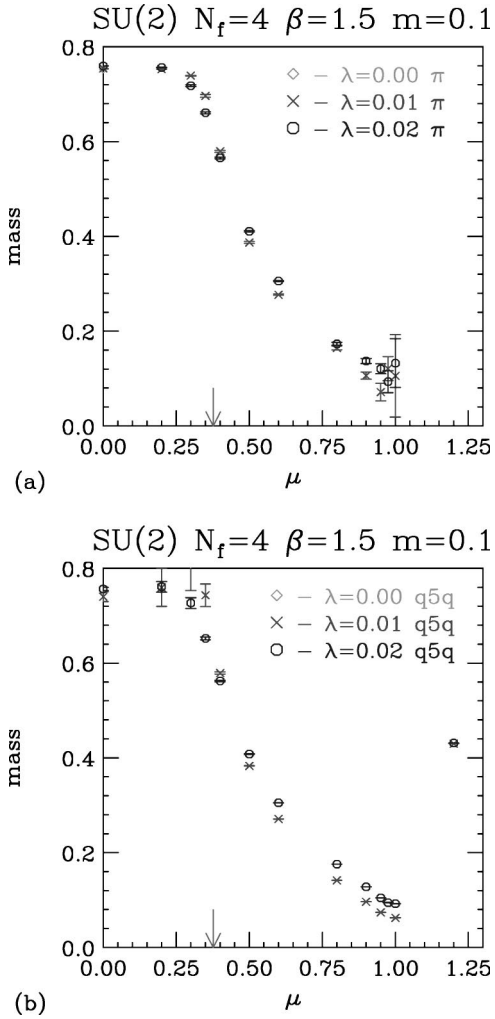

FIG. 6. Pion (a) and pseudoscalar diquark (b) masses as functions of μ.

$$P_\pi(T)=A\{\exp[-m_\pi T]+\exp[-m_\pi(N_t-T)]\} + B(-1)^T\{\exp[-m_{b1}T]+\exp[-m_{b1}(N_t-T)]\} \tag{11}$$

or the form with $B=0$, and a similar form for the diquark state. These masses are plotted in Fig. 6. Note that these 2 graphs are almost identical. For $\mu>\mu_c$, this is expected, since the 2 states mix. For $\mu<\mu_c$ this is not, *a priori*, expected since the diquark state should exhibit a linear decrease with μ for $\lambda=0$. However, since $\lambda\neq 0$ this gives a small mixing with the pion state, which is then the lowest mass particle contributing to this pseudoscalar diquark propagator in this region. It is precisely because this mixing is so small that the errors are so large. The final indicator that this is the correct interpretation was that the $\mu=0$, $\lambda=0$ propagator yielded no sensible mass fit, a sure indicator that the mass was large where there can be no mixing. The pion mass fits in this low μ domain are consistent with the expectation that the $\lambda=0$ pion mass is independent of μ in this region. For $\mu>\mu_c$ these masses fall faster than the expected $m_\pi^2/2\mu$. At least part of the reason for this more rapid falloff is the saturation effect. Note that the reason that this mass tends to zero at large μ (before the saturation transition) is because the pseudoscalar diquark would be a Goldstone boson if $m=0$, and as μ increases the relative importance of m diminishes. The fact that the π mass becomes more poorly determined for large μ is because here, the lowest mass state in this channel is predominantly the pseudoscalar diquark.

It is interesting to contrast our findings with those of a study of adjoint quarks in 2-color QCD [16] with λ set to zero, implying strictly no mixing; in this case m_π was found to rise as $m_\pi\approx 2\mu$ for $\mu>\mu_c$, with the signal becoming appreciably noisier in the high density phase. Both behaviors are in accord with the predictions of chiral perturbation theory for a meson formed from quarks with a symmetric combination of quantum numbers under the residual global symmetry, the difference arising due to the distinct Dyson indices of each model [7].

We now consider the energy densities of the quarks and gluons. Here we limit ourselves to the tree level estimates for these quantities. For the quarks the tree level estimate for the energy density in lattice units is

$$\epsilon_{f0}=\left\langle \bar{\chi}\not{D}_0\chi-\frac{1}{2}+\frac{1}{4}m\bar{\chi}\chi+\frac{1}{4}\lambda\chi^T\tau_2\chi\right\rangle \tag{12}$$

while the gluon energy density is

$$\epsilon_{g0}=\frac{6}{g^2}[\langle P_{ss}\rangle-\langle P_{st}\rangle], \tag{13}$$

where P_{ss} and P_{st} are the traces of the gauge fields around space-space and space-time plaquettes, respectively. We have plotted these quantities in Fig. 7 for the larger, $12^3\times 24$, lattice: those for the 8^4 lattice are similar. What is immediately clear is that the energy density is dominated by the fermion contribution, which contrasts with the finite temperature situation. The gluons only feel the effect of μ due to feedback from the fermion fields, not directly, which helps explain the dominance of ϵ_{f0}. ϵ_{f0} is consistent with zero below μ_c. Above μ_c it rises monotonically towards the saturation value of 1.5. The reason for this is that at very large μ, all that survives in Eq. (12) is the term proportional to e^μ which is identical to the dominant term in j_0, and the $-\frac{1}{2}$. Thus $j_0\rightarrow 2$ implies $\epsilon_{f0}\rightarrow\frac{3}{2}$. ϵ_{g0} is also consistent with zero below μ_c. Above μ_c it rises to a peak at roughly the same μ as does the diquark condensate, and falls as saturation effects turn on. This suggests that the quarks tend to decouple from the gluons when saturation sets in.

Finally we consider the Wilson line (Polyakov loop). Since the $12^3\times 24$ lattice is (to a good approximation) at $T=0$, we expect confinement. Not surprisingly, the measured Wilson line is consistent with zero over the whole range of μ. We expect the 8^4 lattice to be in the low temperature phase at $\beta=1.5$ which is close to the β of the finite temperature transitions for an $8^3\times 4$ lattice at both zero and finite μ. However, since this means that the temperature of this 8^4 lattice, $T\approx 0.5T_c$, we could expect to see some finite temperature effects. This is born out when we examine the Wilson line, which is plotted in Fig. 8. The value of the Wilson

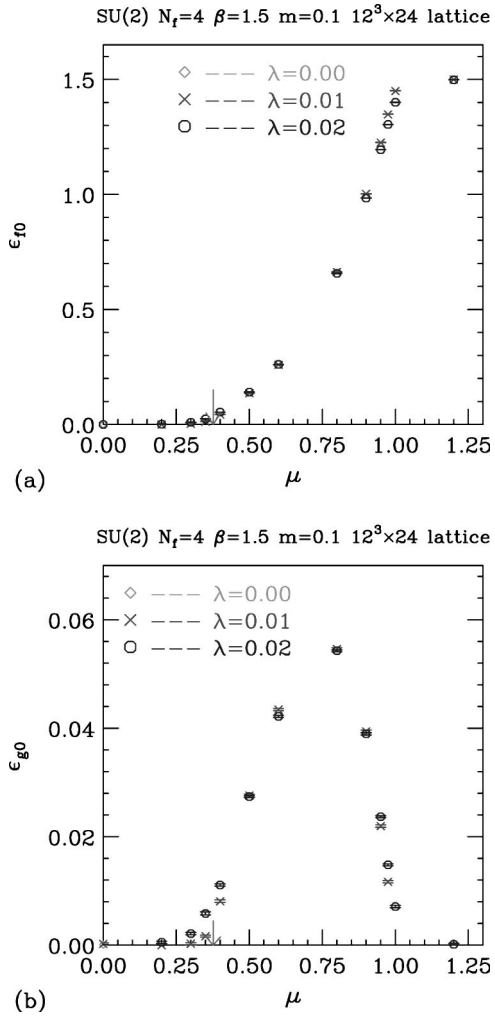

FIG. 7. The (partial) energy densities for (a) the quark and (b) the gluon fields as functions of μ on a $12^3\times 24$ lattice.

line is small (<0.1) over the whole range of μ, consistent with the area law of confinement. It shows no clear signal of the phase transition at μ_c. The drop at the saturation transition indicates that this is not a deconfinement transition, and supports the idea that the quarks are decoupling. Most noticeable is the monotonic rise with increasing μ prior to saturation. This is consistent with the expectation that the finite temperature transition moves to lower temperatures and hence lower β as μ is increased.

IV. CONCLUSIONS

Two-color lattice QCD with one staggered quark species (4 continuum flavors) has been studied at finite chemical potential μ for quark number. We have shown conclusive evidence that this theory undergoes a phase transition to a phase characterized by a diquark condensate which spontaneously breaks the quark number, at $\mu=\mu_c\sim m_\pi/2$. This transition appears to be second order. The simulations were performed at an intermediate value of the coupling (close to β_c for the finite temperature transition at $\mu=0$ on a lattice with $N_t=4$). Because of this, the relevant symmetry was the

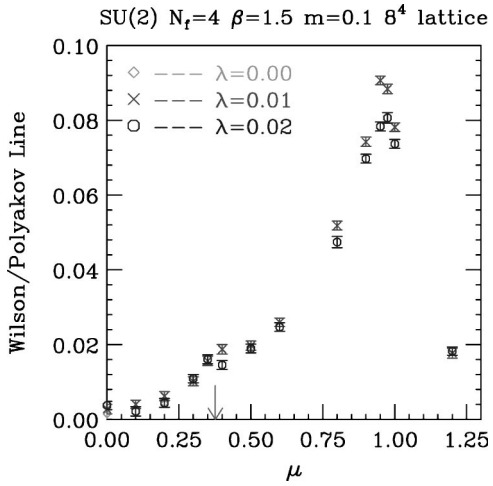

FIG. 8. Wilson line (Polyakov loop) on an 8^4 lattice as a function of μ.

lattice flavor symmetry $U(2)$ rather than the $SU(8)$ of the continuum 4-flavor theory. We have presented convincing evidence that the scalar diquark is the Goldstone boson associated with the spontaneous breaking of quark number for $\mu>\mu_c$. In addition we have measured the lightest mass in the pion channel as a function of μ. For $\mu\lesssim m_\pi$ the chiral condensate and diquark condensate are well described as a single condensate of constant magnitude which rotates from the chiral direction for $\mu<\mu_c$ towards the diquark direction as μ is increased above μ_c. Despite the fact that the quark mass $m=0.1$ was large enough that m_π was not small relative to the 2-color QCD scale, we saw good qualitative agreement with previous calculations in terms of effective Lagrangians (of the chiral perturbation theory form) for $\mu\lesssim m_\pi$. This includes the fact that the quark number density increases from zero at $\mu=\mu_c$.

As μ becomes large, this relationship with effective Lagrangians is no longer valid. Both chiral and diquark condensates decrease towards zero as μ becomes large. However, because at least part of this is due to the fact that j_0 saturates at 2 fermions per site, a finite lattice spacing artifact, and because we see large finite size effects in the condensates for these μ values, studies at smaller lattice spacings as well as on larger lattices would be needed to determine how much of this observed high μ behavior is real.

Our simulations extend the work of [12] and [13] by including the explicit symmetry-breaking Majorana mass term in the simulations themselves, rather than just in the measurements, ensuring that we remain in the correct vacuum. We simulate the 4-flavor theory which presumably has a sensible confining continuum limit, rather than the 8-flavor theory of these earlier papers, which probably does not. We verify the transition to a state in which the quark number is spontaneously broken, reported in these earlier papers. Since the Majorana mass term prevents the Dirac operator from becoming singular in this broken phase due to the presence of Goldstone bosons, we are able to simulate on much larger lattices, allowing us to make accurate measurements of the spectrum of Goldstone and pseudo-Goldstone bosons. (With-

out the Majorana mass term one must rely on the finiteness of the lattice to control the singular behavior of the Dirac operator.) Our graphs for the μ dependence of the condensates and number density are very similar to those obtained by [14] in the strong coupling limit. Since the strong coupling limit is by nature quenched, this contrasts with what is expected for true QCD at finite μ, and is a property of theories that have fermions with both signs for the charge which couples to μ in the same representation of the gauge group —i.e., all the theories we know how to simulate.

We are currently extending these calculations to lower quark mass ($m=0.025$) where we should be able to measure the complete spectrum of Goldstone and pseudo-Goldstone bosons. For this m, the pion mass should be half that at $m=0.1$ and the assumptions of the effective Lagrangian approach should have more validity, allowing a more quantitative analysis. In addition, there is a larger range of μ/m_π between μ_c and the turnover point. This means we can hope to measure the critical index β_{qq} for this transition. (Preliminary attempts to extract this index from short runs at relatively strong coupling were reported in our letter on finite T and μ.) Whereas, in strong coupling, mean field exponents are expected and observed [14], at finite coupling the expectation is less clear. In addition, we plan to study the chiral $m\to 0$ limit, where $\mu_c\to 0$ and the transition becomes first order.

Let us now compare 2-color QCD with 3-color QCD at finite μ. Most of this discussion is condensed from the published literature [4–6]. Since for 2-color QCD, the diquark condensate is a color singlet, the spontaneous breaking of quark number is realized in the Goldstone mode. This contrasts with true (3-color) QCD where the condensate is, of necessity, colored and the symmetry breaking is realized in the Higgs mode. To see similarities, we consider the mode of symmetry breaking for normal QCD with 2 light quark flavors. Here the expected condensate is a flavor singlet and a color anti-triplet, i.e., antisymmetric in both flavor and color. The pattern of color breaking is $SU(3)\times U(1)_q \to SU(2)\times U(1)_Q$ where q and Q refer to the quark number before and after the breaking. The 5 gluons corresponding to symmetries broken by the condensate gain masses via the Higgs mechanism by combining with the 5 would-be Goldstone bosons associated with color and/or quark-number breaking. With respect to the remnant $SU(2)$ color symmetry, the condensate is a flavor *and* color singlet. This is precisely the condensate that would be formed from the 2 quarks which are in a color doublet with respect to this unbroken $SU(2)$ (the third quark is a singlet with respect to this group) if we ignored the interactions of the gluons which gain masses due to the Higgs mechanism. Since the gluon masses produced from the Goldstone bosons produced in this manner are of order $\alpha_s^{1/2}(\Lambda_{QCD})f_\pi$, ignoring such light particle interactions is presumably a rather drastic approximation. However, one might hope that it has at least qualitative validity. [Note that f_π is of the order of 100 MeV, $\alpha_s(\Lambda_{QCD})\sim 1$, giving gluon masses of the same order of magnitude as previous estimates.] Since this remnant $SU(2)$ theory is also at finite μ this condensate spontaneously breaks only 1 symmetry, quark number. As seen above, the Goldstone boson associated with this breaking gives mass to one of the gluons via the Higgs mechanism.

Finally, we note that with an appropriate reinterpretation of the fields, 2-color QCD with a finite chemical potential for the quark number can be reinterpreted as 2-color QCD with a finite chemical potential for isospin. It is clear that one can simulate true 3-color QCD for 2 flavors with a finite chemical potential for isospin. Such a program is underway. The 2-color theory can be used as a guide to the pattern of symmetry breaking and what to expect.

ACKNOWLEDGMENTS

This work was partially supported by the NSF under grant NSF-PHY96-05199 and by the U. S. Department of Energy under contract W-31-109-ENG-38. S.J.H. and S.E.M. were supported by EU-TMR contract no. ERBFMRX-CT97-0122. These simulations were performed on the IBM SP and Cray SV1's at NERSC and on the IBM SP and Cray T90 at NPACI. D.K.S. would line to thank C. K. Zachos for useful discussions.

[1] J. Engels, O. Kaczmarek, F. Karsch, and E. Laermann, Nucl. Phys. B (Proc. Suppl.) **83**, 369 (2000).
[2] B. C. Barrois, Nucl. Phys. **B129**, 390 (1977).
[3] D. Bailin and A. Love, Phys. Rep. **107**, 325 (1984).
[4] M. Alford, K. Rajagopal, and F. Wilczek, Phys. Lett. B **222**, 247 (1998); Nucl. Phys. **B537**, 443 (1999); T. Schäfer and F. Wilczek, Phys. Rev. D **60**, 074014 (1999); **60**, 114033 (1999).
[5] R. Rapp, T. Schafer, E. V. Shuryak, and M. Velkovsky, Phys. Rev. Lett. **81**, 53 (1998).
[6] Good recent reviews include M. Alford, Nucl. Phys. B (Proc. Suppl.) **73**, 161 (1999); E. Shuryak, *ibid.* **83-84**, 103 (2000); K. Rajagopal and F. Wilczek, hep-ph/0011333 (2000).
[7] J. B. Kogut, M. A. Stephanov, D. Toublan, J. J. M. Verbaschot, and A. Zhitnitsky, Nucl. Phys. **B582**, 477 (2000); J. B. Kogut, M. A. Stephanov, and D. Toublan, Phys. Lett. B **464**, 183 (1999).
[8] S. Duane and J. B. Kogut, Phys. Rev. Lett. **55**, 2774 (1985); S. Gottlieb, W. Liu, D. Toussaint, R. L. Renken, and R. L. Sugar, Phys. Rev. D **35**, 2531 (1987).
[9] S. J. Hands, B. Lucini, and S .E. Morrison, Phys. Rev. Lett. **86**, 753 (2001).
[10] S. J. Hands, J. B. Kogut, S. E. Morrison, and D. K. Sinclair, Nucl. Phys. B (Proc. Suppl.) **94**, 457 (2001).
[11] J. B. Kogut, D. Toublan, and D. K. Sinclair, Phys. Lett. B **514**, 77 (2001).
[12] S. Hands, J. B. Kogut, M.-P. Lombardo, and S. E. Morrison, Nucl. Phys. **B558**, 327 (1999).
[13] S. E. Morrison and S. J. Hands, in ''Strong and Electroweak Matter '98','' edited by J. Ambjørn et al., p. 364, hep-lat/9902012; E. Bittner, M.-P. Lombardo, H. Markum, and R. Pullirsch, Nucl. Phys. B (Proc. Suppl.) **94**, 445 (2001).

[14] R. Aloisio, V. Azcoiti, G. Di Carlo, A. Galante, and A. F. Grillo, Phys. Lett. B **493**, 189 (2000); R. Aloisio, V. Azcoiti, G. Di Carlo, A. Galante, and A. F. Grillo, hep-lat/0011079.
[15] W. Pauli, Nuovo Cimento **6**, 205 (1957); F. Gürsey, *ibid.* **7**, 411 (1958); M. E. Peskin, Nucl. Phys. **B175**, 197 (1980).
[16] S. J. Hands, I. Montvay, S. E. Morrison, M. Oevers, L. Scorzato, and J. Skullerud, Eur. Phys. J. C **17**, 285 (2000).
[17] J. B. Kogut, Nucl. Phys. **B290**, 1 (1987).